Optimal-Grade Transition Strategies for Multistage Polyolefin Reactors

Makoto Takeda
SHOWA DENKO K.K.—Oita, Japan 870-0189

W. Harmon Ray
Dept. of Chemical Engineering, University of Wisconsin–Madison, Madison, WI 53706

Polymer-producing companies normally produce many polymer grades in each polymerization reactor train according to customer demands; therefore, many grade-transition operations are necessary. However, the determination of these optimal strategies is difficult. To solve this problem, several sample simulations showing the optimal solutions of grade-transition strategies for multistage olefin polymerization reactors with bimodal products were performed. The methodology utilized a dynamic process simulator, POLYRED, coupled to a sequential quadratic programming, nonlinear optimization algorithm, by using two different objective functions with and without state constraints. It is shown that the most beneficial case of using the optimization technology is the grade transition where the hydrogen content in a reactor must be decreased and/or constraints are imposed on state variables.

Introduction

Today plastic polymers are widely used for various products, such as parts for cars, different kinds of bottles, films, and frames for electric appliances. Each usage requires different specifications for the polymers. In order to satisfy these demands, polymer-producing companies have to produce many different grades of polymers. However, in order to achieve cost saving by operating on a large scale, polymerization processes have very high production capacities and many different grades must be produced in one polymerization process. This requires a special process operation that is called grade transition. In other words, grade transition is an operation whereby one polymer grade is changed to another grade in a polymerization process.

Since grade transition requires drastic and simultaneous changes of different inputs and the dynamics of each input is complicated, multivariable control strategies are necessary in order to cope with the interactions of the inputs. It is very difficult therefore to develop good grade-transition strategies. In most cases, grade-transition strategies are based on previous plant runs that were performed by experienced operators. However, if a reaction process is complicated, as for example, in a multistage process, even experienced operators cannot perform optimal operations, because process dynamics of many inputs must be considered at the same time. In some cases, a step change of each input is performed during grade transitions. However, the residence times of some polymerization reactors (such as loop, tank, and fluidized bed) are normally quite long; therefore, it takes a long time to change over the reactor contents. This leads to a greater amount of off-spec polymers produced during grade transition. Since the difference between the market prices of on-spec and off-spec polymers is quite large, it is very important for a polymer-producing company to perform a good grade-transition operation that produces less off-spec polymer or reduces the production time lost in grade transitions.

Another important aspect of grade transition is plant safety. In order to make a quick changeover in a polymerization reactor, an overshoot and/or an undershoot operation is necessary, but these drastic operations may cause dangerous phenomena such as a runaway reaction in a polymerization reactor.

A product-quality consideration of instantaneous properties is also a very important aspect during grade transitions. For example, instantaneous values for the average molecular weight and/or polymer density should have some upper or

Correspondence concerning this article should be addressed to W. H. Ray.

lower values during grade transitions in order not to produce polymer that has a very high or very low molecular weight and/or density component, because this causes problems in mixing reactor contents and processing polymers.

In order to avoid these phenomena, constraints are imposed during some grade transitions. Hence, when the grade-transition strategy is decided, a good operation that minimizes grade-transition time or amount of off-spec polymer should be considered while satisfying product constraint.

One tool for obtaining good grade-transition strategies is to make dynamic simulations by using dynamic kinetic and process models. The performances of several different strategies are easily simulated and some process constraints can also be checked. Ramanathan and Ray (1991) made dynamic simulations of grade transition for two fluidized-bed reactors, and Debling et al. (1994) simulated grade-transition operations for various kinds of polymerization processes. In both studies, they compared the performance of many different grade-transition strategies and calculated the amount of off-spec product. However, because in these simulations trial-and-error methods were adopted to get a good grade-transition strategy, it is time-consuming to use this method and to find an optimal grade-transition strategy. Accordingly, obtaining an optimal grade-transition strategy more efficiently is the main motivation of this article.

Another tool for obtaining a good grade-transition strategy is to solve a dynamic model-based optimization problem. McAuley and MacGregor (1992) obtained optimal grade-transition strategies in a gas-phase polyethylene reactor by solving the optimization for a lumped-parameter system. Although the constraints for input variables were considered in their article, the constraints for the state variables were not considered. Ohshima et al. (1994) also conducted optimal grade-transition strategies in a loop and gas-phase polypropylene reactor by using dynamic programming after simplifying the correlation models of polypropylene specifications.

In McAuley's and Ohshima's articles, correlation models among Melt Index, density, and gas concentrations in the reactor were used. Although these correlation models make solving optimizations easier, they cannot represent other polymer specifications such as polydispersity and chain-length distribution. If the dynamics and/or constraints of the detailed polymer specifications must be considered during grade transition, more complicated kinetic models should be used.

In this study, to overcome the weaknesses described earlier, optimization of grade-transition strategies is performed, while considering the following points. First of all, more complicated kinetic models than correlation models are used for calculating polymer specifications. Second, by using these models, several grade-transition optimization problems are solved with and without some constraints for state variables, and the results are compared in order to discover which cases yield practically useful results. Third, the decision variables in optimization are reduced and compared with more complex optimization. Finally, a different objective function considering a product band is used and the performance is compared. Specifically, the control-vector parameterization method is used to solve the dynamic process optimizations. Successive quadratic programming (SQP) is selected as an algorithm to solve optimization with constraints, and the dynamic simulation package POLYRED (UWPREL, 1997) is used for dynamic process and polymer kinetic modeling.

Grade-Transition Trajectory Optimization

Optimization problem formulation

When grade transitions are dealt with, a process model (inputs, states, and outputs) must be included in the optimization formulation. To have the best process dynamics under a certain objective function is a goal of grade-transition optimization; thus, the optimization must calculate the best input trajectory during grade transition, considering the trajectories of states and outputs. This requires that the trajectories of inputs, states, and outputs, which are the functions of the parameter time t, be included in an objective function and constraints of the optimization problem.

The general formulation of the grade-transition optimization problem can be written as

$$\begin{aligned} &\min_{\underline{u}(t)} F[u(t), x(t)] \qquad t \in [t_0, t_f] \\ &\text{s.t. } c[u(t), x(t)] = 0 \\ &\frac{dx}{dt} = f[u(t), x(t)] \\ &x(t_0) = x_0 \\ &u_{\text{low}} \le u(t) \le u_{\text{up}} \\ &x_{\text{low}} \le x(t) \le x_{\text{up}} \end{aligned} \tag{1}$$

where $x(t)$ is the m-dimensional state vector and $u(t)$ is the n-dimensional input vector. In this problem the decision variables are the inputs $u(t)$ and the differential equations that show process dynamics are included in the constraints. Normally in the objective function the integration of $x(t)$ is included. The two main differences between this type of problem and the standard NLP are:

1. The time variable t is included in the objective function and constraints.
2. The constraints include differential equations.

Because of difference 1, this type of optimization problem is called a trajectory optimization problem. In solving the trajectory optimization problem, difference 2 makes this problem difficult to solve directly. Therefore, it is not easy to directly use the standard optimization theory and algorithms in order to solve this type of problem. Although there are several methods, such as control-vector iteration procedures, direct substitution approaches, dynamic programming, and control-vector parameterization (Ray and Szekely, 1973), to deal with this problem, the control-vector parameterization is used in this article because it is easy to install a complicated process model and to have constraints involving state variables.

Control-vector parameterization

Control-vector parameterization is an algorithm for solving dynamic optimization problems by changing the decision variables from time-varying process inputs $u(t)$ to parame-

ters, for example, by using the following equation:

$$u_i(t) = \sum_{j=1}^{s} a_{ij}\phi_{ij}(t). \tag{2}$$

Here $u_i(t)$ is the ith element of the input vector of $u(t)$, ϕ_{ij} is a trial function, and the parameters a_{ij} are the decision variables that are optimized in the control-vector parameterization. In this method the trial functions ϕ_{ij} must be determined first. This approach has the main advantage of being able to eliminate the time parameter t and converting the optimization problem to the following parameter estimation problem:

$$\begin{aligned} &\min_{a_{ij}} F(a_{ij}) \\ &\text{s.t. } g(a_{ij}) \le 0 \\ &\quad h(a_{ij}) = 0. \end{aligned} \tag{3}$$

In Eq. 3, the decision variables are new parameters a_{ij}, and the time domain can be eliminated from Eq. 1. The trial functions, $\phi_{ij}(t)$, can be polynomials or other classes of functions; alternatively, they can be a series of step changes. The objective function F, inequality constraint function g, and equality constraint function h are the functions of a_{ij}. Actually, this is the same formulation for standard NLP. Now that Eq. 1 is converted to Eq. 3, any algorithms for solving the standard constrained NLP can be applied to solve Eq. 3. When Eq. 3 is solved with NLP algorithms, the values of the functions F, g, h and their gradient ∇F, ∇g, ∇h with regards to a_{ij} are necessary at every step. For example, in SQP, these values are necessary when the QP subproblem is solved. In the control-vector parameterization, these values are obtained by performing a dynamic process simulation and using the finite difference method. Because parameters a_{ij} at iteration k are obtained and the input series $u(t)$ can be calculated with a_{ij} and trial functions ϕ_{ij}, the dynamic process model simulations for a nonlinear model can be performed; therefore, a special model is not necessary in solving the optimization problem.

The control-vector parameterization approach is shown in Figure 1. The algorithm consists of four main procedures:

- Calculate the process input $u(t)$ from the a_{ij} and $\phi_{ij}(t)$.
- Perform dynamic process simulations.
- Calculate the values of F, g, h and their derivatives.
- Use an NLP optimization algorithm to determine improved values for the a_{ij}.

These four procedures are connected and performed sequentially; starting with the initial guesses for parameters a_{ij}, the inputs $u(t)$ are calculated and input to the dynamic process simulator. The values of the states at each time are output from the dynamic process simulator, and the values of the corresponding functions and derivatives are calculated and input into an optimization algorithm. By using the new parameters, which are output from the optimization algorithm, as the next iteration values, the new inputs are calculated and input to the dynamic process simulator again. In this article SQP in MATLAB (Grace, 1992) is used as the optimization algorithm and POLYRED (UWPREL, 1997) is used as a dynamic process simulator.

The advantages of the control vector parameterization are:

1. One can use the standard optimization algorithms.
2. Even if a process model is very complicated, the optimization solution can be obtained using existing process simulators.

However, it is important to select $\phi_{ij}(t)$ well; if these functions are poorly chosen, the solution may not necessarily be optimal.

Process Description

In this article, by using Ziegler-Natta transition-metal catalyst, the slurry-phase loop reactor is used for simulations. The loop reactor consists of a main tubular system closed in a loop. The reaction mixture flows through the tube, impelled by an axial pump. In the bimodal loop reactor, two loop reactors are serially connected. By setting different reaction conditions in each reactor, polymers with broader molecular-weight distribution can be produced. The typical bimodal loop reactor is shown in Figure 2. A diluent is fed to both reactors as a liquid. Ethylene as a main monomer is fed to both reactors, and hexene as a comonomer is fed only to the first reactor; as a result, high-density polyethylene is produced in this reactor. The density of polymer in both reactors is controlled

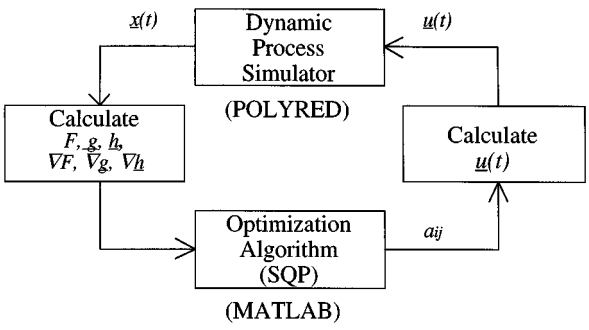

Figure 1. Control vector parameterization.

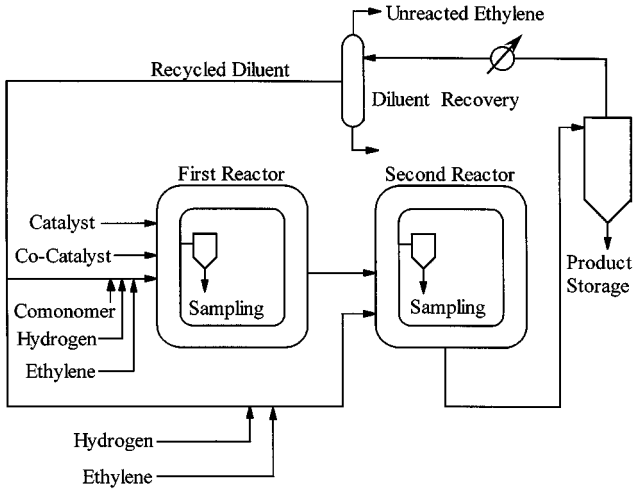

Figure 2. Bimodal loop reactors.

by a comonomer. Hydrogen as a chain transfer agent is fed to both reactors in order to control the molecular-weight distribution. A transition-metal Ziegler-Natta catalyst is fed to the first reactor with alkyl as a cocatalyst.

Each loop is enclosed by a jacket in which the coolant water flows. Reactor temperature is controlled by adjusting the coolant temperature. Reactor pressure is controlled by changing the discharge amount from the reactor. The mixture that is discharged from the reactor is sent to the separator, where the diluent with the unreacted monomer and polymers are separated. The separated polymers are dried and sent to the storage tank. The mixture of diluent and the unreacted monomer is sent to the distillation column, where the diluent is purified. The purified diluent is recycled to feed the reactors again. In this process polymer samples can be taken from the first and the second reactor, and the samples obtained from the second reactor can be regarded as the final product. Because these two samples can be measured directly, the main specifications of polymers are those of the first-reactor product and those of the final product.

Regarding the specifications that determine the properties of polymers, molecular-weight distribution and polymer density are the most important specifications of industrial polyolefin products, because they have a big effect on polymer processability and stiffness. Since it is difficult to express the molecular-weight distribution directly, the number- or weight-average molecular weight (Melt Index is often used for showing these properties) and polydispersity are used to show the molecular-weight distribution of polymers; therefore, the number-average molecular weight, polydispersity, and polymer density are the main specifications of polymers in the sample simulations.

The product from these tandem reactors has a bimodal molecular-weight distribution (cf. Figure 3) where one mode is produced in each reactor. Thus the process is often called a *bimodal process*. For the process considered here the higher molecular-weight mode is produced in the first reactor and the lower molecular-weight peak in the second reactor. Thus the product is a bimodal high-density polyethylene (HDPE).

Mathematical Model for Bimodal Reactors

In performing dynamic process simulations, some assumptions for a process and kinetics are made to simplify the calculations.

The assumptions in process modeling are:

1. Each loop reactor can be regarded as a continuous stirred-tank reactor (CSTR) because the recycle rate in the reactor is very high (Zacca and Ray, 1993).

2. The reactor temperature is perfectly controlled at the setpoint.

3. The reactor pressure is controlled by overflowing the reaction mixtures from the reactors.

4. There are no impurities in the reactors.

5. The reactions that produce byproducts (such as ethylene + hydrogen → ethane) are not considered.

The assumptions for the kinetics of Ziegler-Natta polymerization reactions are:

6. The number of the catalyst sites is two.

7. Site activation by cocatalyst and comonomer, chain initiation by monomer, chain propagation by monomer, chain transfer by hydrogen and monomer, spontaneous chain transfer, and spontaneous site deactivation are considered.

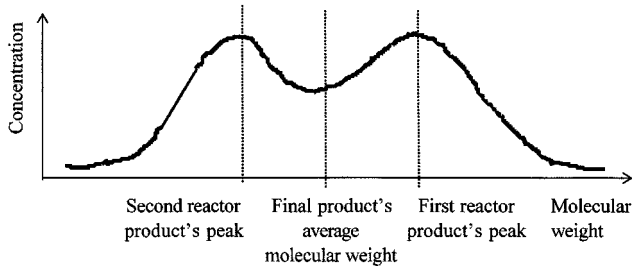

Figure 3. Bimodal molecular-weight distribution.

8. Chain transfer is performed only at the same site. That is, there is no chain transfer from site 1 to site 2 nor from site 2 to site 1.

9. There are some sites in the catalyst that are activated only by a comonomer (Karol et al., 1993).

10. There are two types of site initiations: the initiation after performing chain transfer and the initiation from the potential sites. The former takes a longer time than the latter (Shaffer and Ray, 1997).

In the preceding, assumptions 1, 9, and 10 are validated in the corresponding references. Generally the remaining assumptions are valid, but they depend on the characteristics of each catalyst and process. Even if additional kinetics are necessary, however, they can be installed in a dynamic process simulator, and the optimization problem can be easily solved through the use of control vector parameterization. The kinetic parameters for the simulations are given in Table 1, and detailed modeling equations are described in the Appendix.

The Optimization Examples

In this section, the example grade transitions, the specific objective function, control-vector parameterization, and other specifications of the optimization examples are presented. First of all, the three steady states in Table 2 (A, B, C), representing three grades of polymer, are considered in the simulations. Among these three steady states, the following grade-transition operations are optimized:

1. From steady-state A to steady-state B
2. From steady-state B to steady-state C.

Grade transition 1 is an easy grade transition because flows other than the first hexene and the first and second hydrogen flows are constant before and after the grade transition. Grade transition 2 is difficult because almost all flows must be changed before and after the grade transition. In other words, grade transition 1 requires only a change in the number-average molecular weight and polymer density. By contrast, the production rate and production-rate ratio between the first and second reactors must be changed in grade transition 2.

In practice, certain economic objectives are used as goals for grade transitions. For example:

1. When polymer sales are high and the plant is operating at maximum capacity, one usually wishes to minimize the time of the grade transition so as to keep the plant production rates as high as possible.

Table 1. Kinetic Constants*

	Site 1	Site 2
Activation energy (chain transfer) (cal/mol)	14,000	14,000
Activation energy (others) (cal/mol)	9,000	9,000
Site activation constant (L/mol·s)		
By cocatalyst	7.0×10^5	7.0×10^5
By hexene	1.0×10^6	1.0×10^6
Chain initiation constant (L/mol·s)		
By ethylene	2.7×10^6	2.7×10^6
By hexene	3.8×10^5	3.8×10^5
Chain propagation constant (L/mol·s)		
By ethylene end-gr. = ethylene	2.0×10^8	2.0×10^8
By ethylene end-gr. = hexene	1.7×10^8	1.7×10^8
By hexene end-gr. = ethylene	5.0×10^6	2.0×10^6
By hexene end-gr. = hexene	4.0×10^5	8.4×10^5
Chain transfer constant (L/mol·s)		
By hydrogen end-gr.-ethylene	3.0×10^7	3.2×10^8
By cocatalyst end-gr. = ethylene	6.0×10^5	3.0×10^6
Spontaneous end-gr. = ethylene**	2.8×10^2	2.8×10^2
By ethylene end-gr. = ethylene	6.0×10^5	6.0×10^5
By hexene end-gr. = ethylene	1.0×10^7	1.6×10^8
By hydrogen end-gr. = hexene	3.0×10^7	3.2×10^8
By cocatalyst end-gr. = hexene	1.3×10^6	6.0×10^5
Spontaneous end-gr. = hexene**	2.8×10^2	2.8×10^2
By ethylene end-gr. = hexene	6.0×10^5	6.0×10^5
By hexene end-gr. = hexene	1.0×10^7	1.6×10^8
Site deactivation constant		
Spontaneous**	3.0×10^2	3.0×10^2

*Constants are pre-exponential factors.
**Units are s^{-1}.

Table 2. Three Sample Steady States

	Steady States A	Steady States B	Steady States C
1st reactor volume (m^3)	10.0	10.0	10.0
2nd reactor volume (m^3)	30.0	30.0	30.0
1st reactor temperature (degree *c*)	90.0	90.0	90.0
2nd reactor temperature (degree *c*)	90.0	90.0	90.0
1st C_6 flow (g/s)	25.0	50.0	95.0
1st H_2 flow (g/s)	0.1	0.2	0.1
2nd H_2 flow (g/s)	12.0	3.0	15.0
1st C_2 flow (g/s)	1,667.0	1,667.0	2,292.0
2nd C_2 flow (g/s)	1,667.0	1,667.0	1,910.0
1st Dil. flow (g/s)	2,222.0	2,222.0	2,222.0
2nd Dil. flow (g/s)	1,111.0	1,111.0	1,800.0
1st Cat. flow (g/s)	0.17	0.17	0.21
1st Cocat. flow (g/s)	0.10	0.10	0.10
1st Inst. MW_n	53,822	35,221	56,316
1st Cumu. MW_n	53,783	35,175	56,237
1st *Zp*	6.1	6.3	6.5
1st Inst. density	0.9462	0.9411	0.9377
1st Cumu. density	0.9462	0.9411	0.9377
2nd Inst. MW_n	6,899	9,280	7,504
Final Cumu. MW_n	12,079	14,515	14,143
Final Cumu. *Zp*	15.4	9.6	15.5
2nd Inst. density	0.9501	0.9454	0.9445
Final Cumu. density	0.9481	0.9431	0.9402
1st production rate (g/s)	1,629	1,636	2,272
2nd production rate (g/s)	1,629	1,666	1,859
Production rate ratio	50:50	49.5:50.5	55.0:45.0
Total production rate (g/s)	3258	3302	4130
1st wt. frac. polymer	0.416	0.415	0.493
2nd wt. frac. polymer	0.486	0.491	0.496
1st residence time (H)	0.418	0.415	0.372
2nd residence time (H)	0.765	0.767	0.617

2. When polymer sales are low and the plant is operating at reduced capacity, one usually wants to minimize the amount of off-spec product produced (even if this extends the transition time) because one may have difficulty in selling the off-spec product.

In other situations, even more specific objectives could be important.

In this work, we chose as our objective a time-weighted least-squares objective (cf. Eq. 4) because other optimal control studies (Ogunnaike and Ray, 1994) have shown that this objective provides very useful practical results. It selectively penalizes both large deviations as well as long-time deviations from the target. While later studies will use a greater variety of objective functions, this first study illustrates the types of grade-transition strategies found by the optimizer and the degree of practical improvement over simpler strategies.

Our first objective function to be tested is

$$F=\int_{t_0}^{t_f}\left\{w_1*t*\left(\frac{1MW_n(t)-1MW_nT}{1MW_nT}\right)^2+w_2*t*\left(\frac{1\rho(t)-1\rho T}{1\rho T}\right)^2+w_3*t*\left(\frac{1Zp(t)-1ZpT}{1ZpT}\right)^2+w_4*t*\left(\frac{FMW_n(t)-FMW_nT}{FMW_nT}\right)^2+w_5*t*\left(\frac{F\rho(t)+F\rho T}{F\rho T}\right)^2+w_6*t*\left(\frac{FZp(t)-FZpT}{FZpT}\right)^2\right\}dt. \quad (4)$$

In Eq. 4, $1MW_n$ and FMW_n are the number average molecular weight in the first and second (final) reactors, respectively, and $1MW_nT$ and FMW_nT are their target values. Similarly, 1ρ and $F\rho$ are the polymer density in the first and second reactor, and their target values are $1\rho T$ and $F\rho T$; $1Zp$ and FZp are the polydispersity in the first and second (final) reactors, respectively; $1ZpT$ and $FZpT$ are their target values; and $w_1 \sim w_6$ are the weight factors. Because the specifications of the final product are more important than the first reactor product, the larger values are set to w_4, w_5, and w_6. However, because the final product bimodal MWD and composition distributions depend critically on the model produced in the first reactor, one cannot ignore the weights w_1, w_2, w_3. The instantaneous molecular weight and density in the first and second reactors are not measured directly; therefore, these are not included in the objective function, although they may be considered as constraints.

Although the objective function, Eq. 4, produces fast grade transitions without excessive overshoot/undershoot, each polymer property has only one target value ($1MW_nT$, FMW_nT, $1\rho T$, $F\rho T$, $1ZpT$ and $FZpT$). However, it is quite common in practice that the target values of each grade have a band, that is, the target of each property has an upper and lower bound. If the product is within this band, it is on-spec, and if not, it is off-spec. Normally the target values in the objective function, Eq. 4, are the center values of the on-spec band. Hence, the objective function, Eq. 4, does not necessarily give the least off-spec product. Accordingly, another objective function, Eq. 5, is proposed so as to include the product band, and optimization is performed to compare the results with Eq. 4. In this optimization, Zp is not included for simplicity.

$$F = \int_{t_0}^{t_f} \{ t * (P_1 + P_2 + P_3 + P_4) \}\, dt \tag{5}$$

where

$$P_1 = \begin{cases} w_7 * \left(\dfrac{1MW_n(t) - 1MW_nT}{1MW_nT} \right)^2 \\ \qquad \text{if } 1MW_n(t) \text{ is within the band.} \\ w_{11} * \left(\dfrac{1MW_n(t) - 1MW_nB}{1MW_nB} \right)^2 \\ \qquad \text{if } 1MW_n(t) \text{ is outside the band.} \end{cases}$$

$$P_2 = \begin{cases} w_8 * \left(\dfrac{1\rho(t) - 1\rho T}{1\rho T} \right)^2 & \text{if } 1\rho(t) \text{ is within the band.} \\ w_{12} * \left(\dfrac{1\rho(t) - 1\rho B}{1\rho B} \right)^2 & \text{if } 1\rho(t) \text{ is outside the band.} \end{cases}$$

$$P_3 = \begin{cases} w_9 * \left(\dfrac{FMW_n(t) - FMW_nT}{FMW_nT} \right)^2 \\ \qquad \text{if } FMW_n(t) \text{ is within the band.} \\ w_{13} * \left(\dfrac{FMW_n(t) - FMW_nB}{FMW_nB} \right)^2 \\ \qquad \text{if } FMW_n(t) \text{ is outside the band.} \end{cases}$$

$$P_4 = \begin{cases} w_{10} * \left(\dfrac{F\rho(t) - F\rho T}{F\rho T} \right)^2 & \text{if } F\rho(t) \text{ is within the band.} \\ w_{14} * \left(\dfrac{F\rho(t) - F\rho B}{F\rho B} \right)^2 & \text{if } F\rho(t) \text{ is outside the band.} \end{cases}$$

Here the designation B denotes the upper limit if the trajectory is over the upper limit, and the lower limit if the trajectory is under the lower limit. This objective function considers two different regimes. If the current value is outside the band, the target value is set to the nearest band (upper or lower) of the product. Once it goes into the product band, the target value is changed to the center value of the property. Because on-spec means the polymer has all properties inside the property band, larger values are used for the weight factors for outside the band ($w_{11} \sim w_{14}$) in order for every property to go into the property band quickly. Once each property goes into the property band, it gradually goes toward the center value, because the weights $w_7 - w_{10}$ are smaller. This has the practical effect that the optimizer can always focus most of the control effort on those properties that are outside the band.

The controlled variables during grade transition are the hexene flow to the first reactor, the hydrogen flow to the first reactor, and the hydrogen flow to the second reactor. In all simulations, these inputs have upper and lower constraints. The upper constraints are set to 1.5*(the value of the steady state after grade transition), and the lower constraints are set to zero. Although simulations that have no state constraints are referred to as no constraints, all simulations have these input constraints. In simulation 2, ethylene and catalyst flows are ramp changed, because too rapid changes of these variables can cause reactor heat-removal problems. Both ethylene feeds to the first and second reactors are ramp changed, keeping the production-rate ratio between the first and second reactors constant.

Finally, the control-vector parameterization of the three controlled variables is shown in Figure 4. The parameterizations by the solid line in Figure 4 are usually used. For each variable, time is divided into some intervals, and in each interval the input is kept constant. Because the dynamics of each controlled variable are different, each has a different number of intervals. For example, the dynamics of the number-average molecular weight in the first reactor is faster than that of the second reactor; hence, the number of intervals in the first reactor hydrogen flow is five, while that of the second reactor hydrogen is eight. For each controlled variable, the length of each interval is set differently. This is because at the beginning of the grade transition, frequent input changes are necessary in order to have a better result, but at the end of the grade transition, the process is close to the steady state and frequent changes are not necessary. The grade transition starts at $t = 900$ s in every simulation, and before $t = 900$, the inputs remain at the steady-state values of the previous grade. The steady-state values of the new grade are set after the final parameterized input. The time when this value is set is different in each input. The initial values of the control-vector parameterization are set to the steady-state values of the new grade. This means the optimization starts from the step change of inputs.

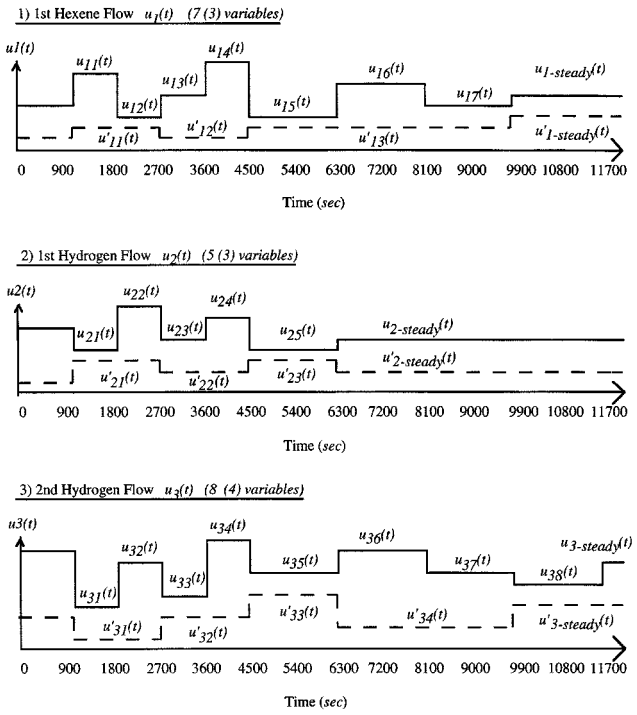

Figure 4. Parameterization of inputs.

Dashed lines are the reduced parameterizations of the inputs, which are compared to the results with normal solid-line parameterizations.

Optimization Results

Easy grade transitions

Easy grade transitions (grade transition 1), during which only the first hexene flow, the first hydrogen flow, and the second hydrogen flow are dynamically changed, are optimized under the two different objective functions: in the first simulation Zp is included and the other one has no Zp in the objective function (that is, w_3 and w_6 in Eq. 4 are set to zero). The final results are shown in Figures 5–8. In these figures, the instantaneous number-average molecular weight (Inst. MWn) and cumulative number-average molecular weight (MWn) and polymer density of the first reactor, the instantaneous number-average molecular weight (Inst. MWn) and polymer density in the second reactor, the cumulative number-average molecular weight (MWn) and polymer density of the final product, polydispersity (Zp) of the first reactor and the final product, and the optimized inputs, that is, the hexene flow to the first reactor (C_6 flow), the hydrogen flow to the first and second reactors (H_2 flow), are shown. In order to distinguish the first reactor, second reactor, and the final products, the symbols 1 (for the first reactor), 2 (for the second reactor), and F (for the final product) are added in front of each symbol of the calculated variable. The following four simulations are conducted for each grade transition:

a. The step-change operation (dashed lines).

b. The unconstrained optimization results including Zp in the objective function (dotted lines).

c. The unconstrained optimization results without Zp in the objective function (solid lines).

d. The constrained optimization results without Zp in the objective function (dot-dash lines). The constraints are: the first instantaneous density ≥ 0.940; the second instantaneous density ≥ 0.945.

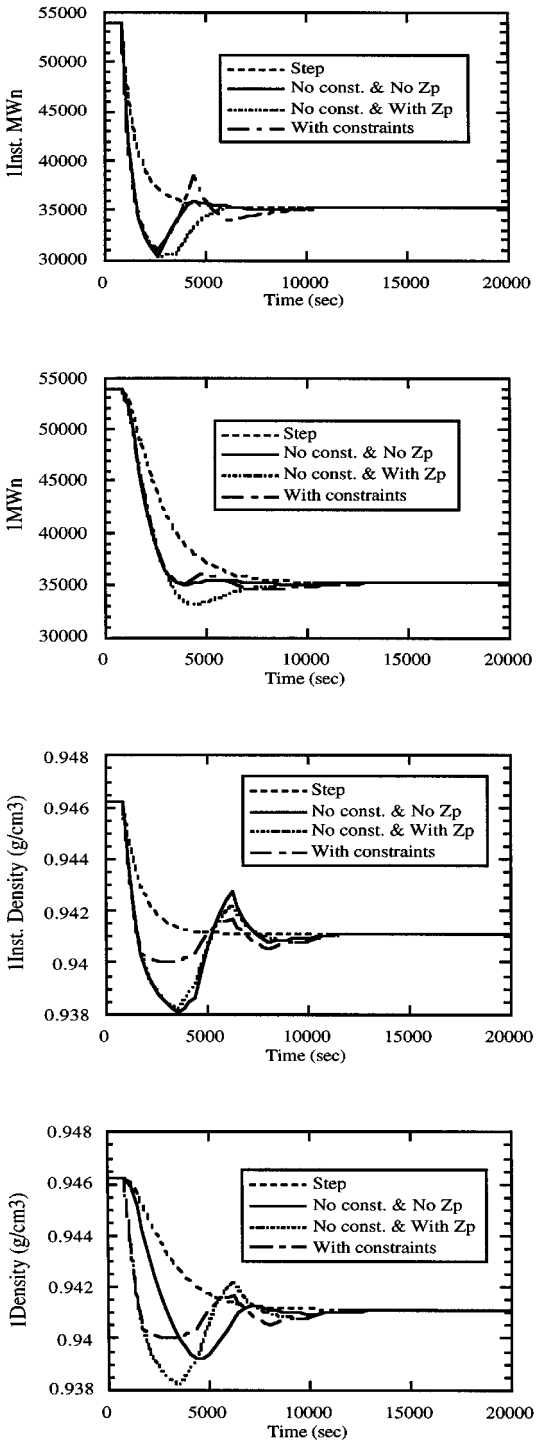

Figure 5. Results of easy grade transition—(1).

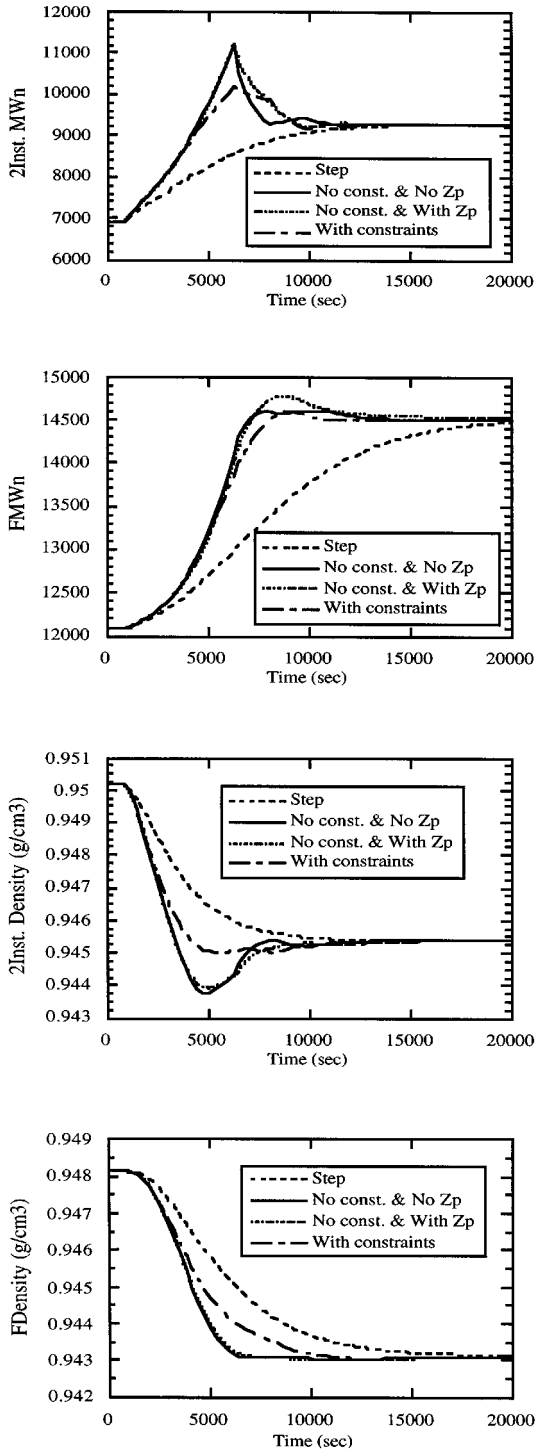

Figure 6. Results of easy grade transition—(2).

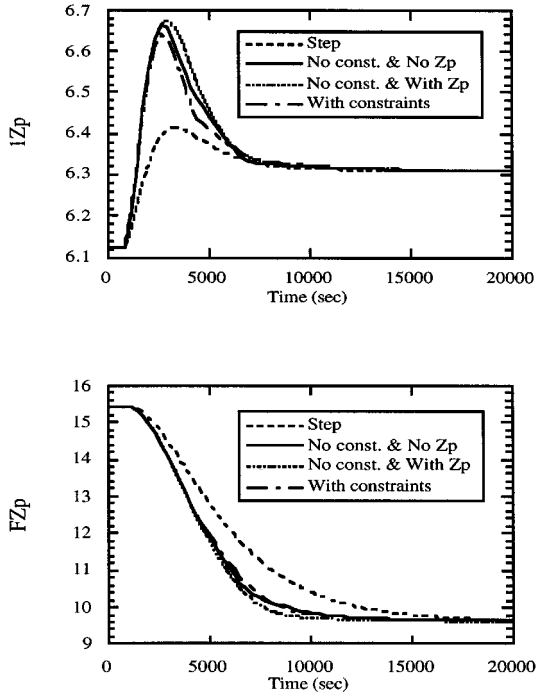

Figure 7. Results of easy grade transition—(3).

These four results are shown in the same graph in order to easily compare the optimization results. In these simulations the results may be summarized as follows.

First, the grade-transition time is much improved from the step change in optimized grade transition by overshooting/undershooting the instantaneous values. Note that in optimization Case d the constraints are completely satisfied. More important, the cumulative value of the polymer density in the first reactor is also overshot/undershot in order for the polymer density in the final product to change quickly. This means that the optimization can calculate the synchronized solutions between the first and second reactors. Although the polydispersity in the first reactor is more overshot in the optimization results, the degree of the overshooting is not very high and this can be allowed during grade transitions.

Second, the inclusion of Zp in the objective function has a trade-off effect with the dynamics of the cumulative number-average molecular weight, and it is possible to use this objective function for a grade transition in which Zp is very important. However, the progress in dynamics of the first and final Zp is not significant in this optimization. Therefore, in some later optimizations, Zp is not included in the objective function for simplicity.

Finally, the optimized results of each flow have a common pattern in the unconstrained optimization. Each should be increased (decreased) to the upper (lower) bound and decreased (increased) under (over) the final steady state's value and return to the steady state's value. These solutions are not very surprising and in practice these operations can be performed by experienced operators. The solutions for the constrained optimization are more interesting and are not easily performed by experienced operators. Hence, it is more beneficial to conduct grade-transition optimization for constrained grade transitions.

Difficult grade transition

The following optimizations are performed for grade transition 2:

e. Step-change operation (dashed line).
f. Unconstrained optimization (solid line).
g. Constrained optimization (dotted line).

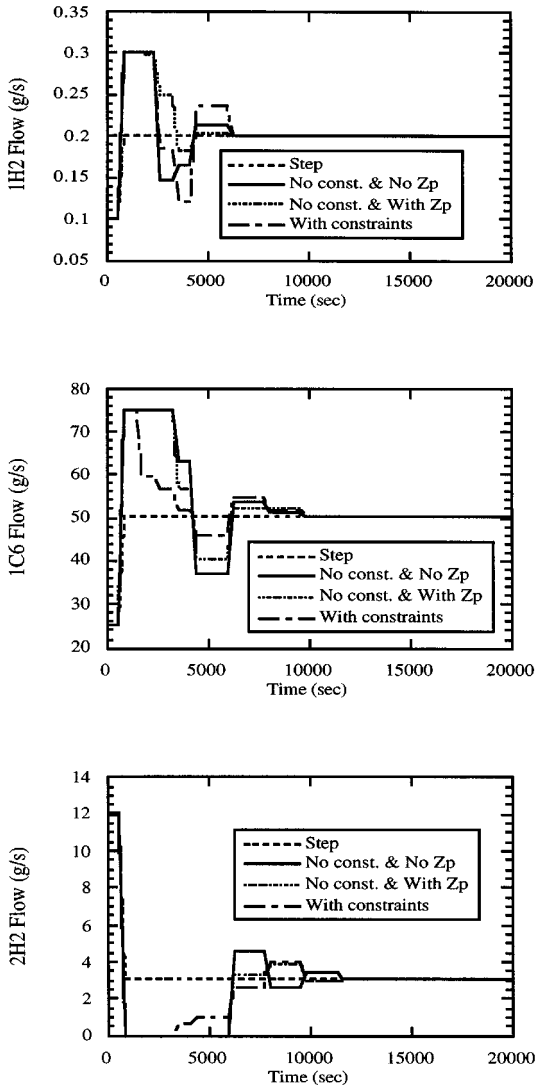

Figure 8. Results of easy grade transition—(4).

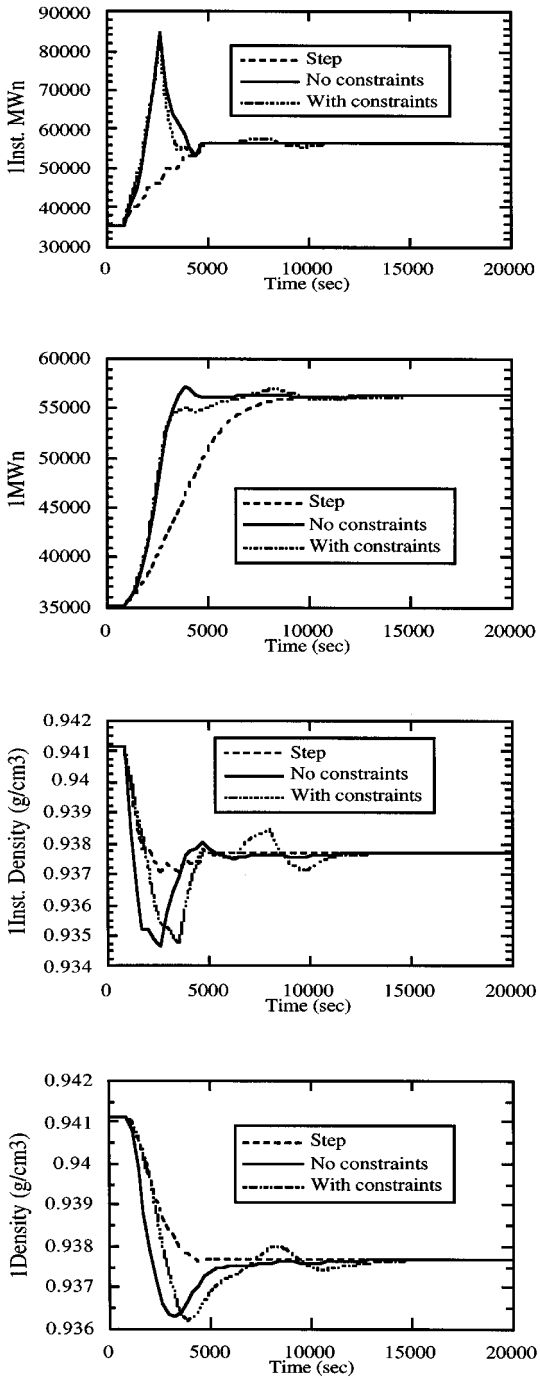

Figure 9. Results of difficult grade transition—(1).

The results are shown in Figures 9–12. In these figures the same variables as those in easy grade transition and the production rates in both reactors are included because production rates in both reactors are increased. (In order to see it clearly, the time span in the graph of production rate is different from others.) The optimized controlled variables are the first reactor hexene flow, and the first and second reactor hydrogen flows. The ethylene flows to both reactors and the catalyst flows to the first reactor are changed as a ramp, and the diluent flow to the second reactor is a step change, as shown in Figure 13. The diluent flow and cocatalyst flow to the first reactor are kept constant.

For unconstrained optimization of the difficult grade transition, the following interesting results can be obtained. First, grade-transition time is much improved compared with the step change. The instantaneous values and the cumulative density in the first reactor are adjusted to have very rapid dynamics for the final product values. The polydispersity in the first reactor is overshot, but this is not a big overshoot compared to the steady-state value. These results are very similar to those of easy grade-transition cases.

Second, although the hexene flow and hydrogen flow to the first reactor have expected dynamics, that is, they go to the upper or lower constraints and return to some points close to the steady states, the optimized result of the second reactor hydrogen flow is quite different especially at the beginning of the grade transition. This can be explained as follows: while the production rate of the first reactor is not increased, the hydrogen flow to the second reactor is changed mainly to

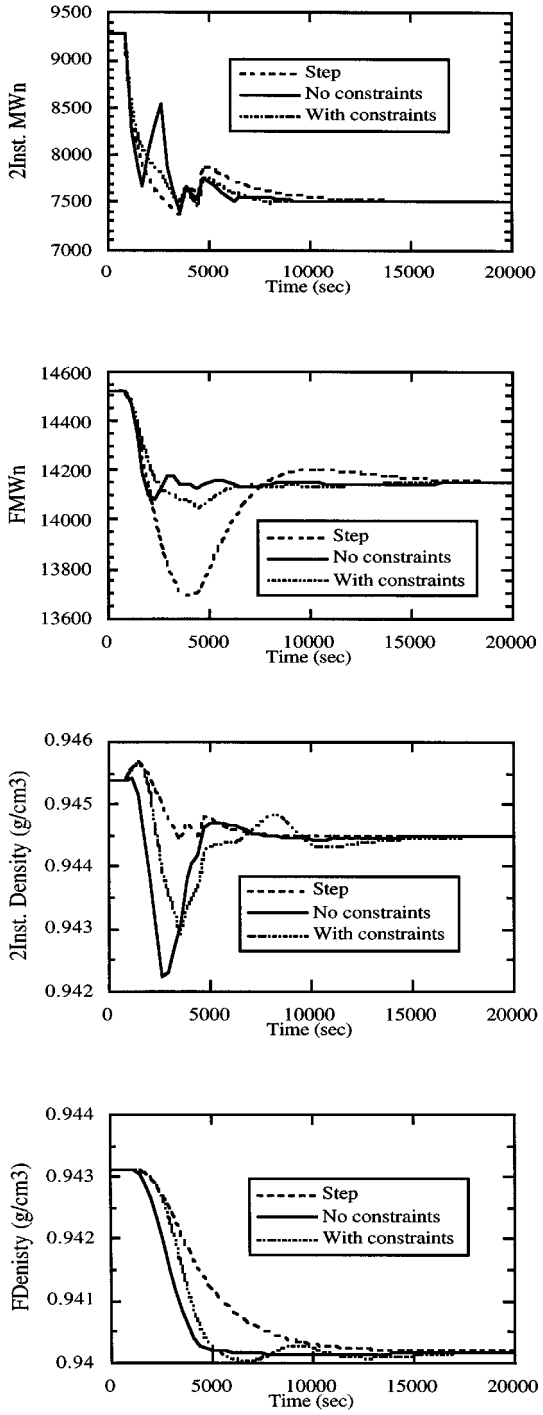

Figure 10. Results of difficult grade transition—(2).

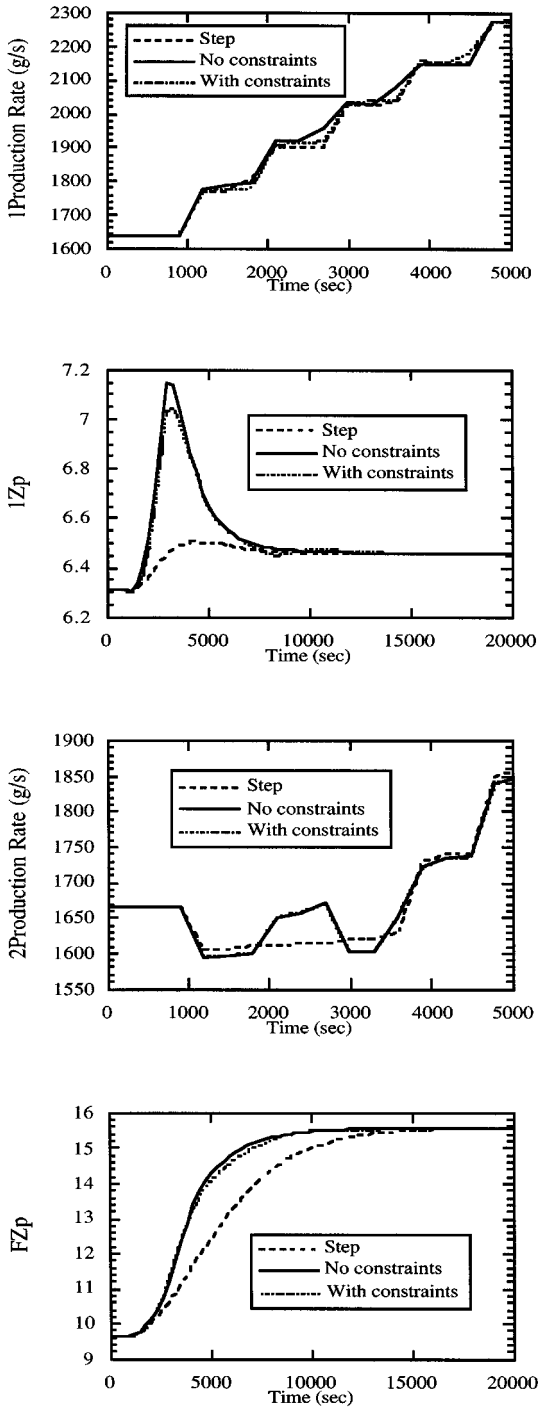

Figure 11. Results of difficult grade transition—(3).

have a rapid decrease in the number-average molecular weight in the second reactor; therefore, a rapid increase and decrease of the second hydrogen flow is performed at the beginning of the grade transition in order not to have an undershoot of the number average of molecular weight, as in the step-change case. As the production rate of the first reactor is increased, the hydrogen flow to the second reactor is greatly increased at $t = 2{,}700$ s, producing lower instantaneous number-average molecular weight in the second reactor, because polymer with a high number average of molecular weight is coming from the first reactor. The hydrogen flow to the second reactor is increased again at $t = 4{,}500$ s as the production rate in the second reactor is increased.

Although there are several disturbances to the number-average molecular weight and polymer density, such as increasing catalyst concentration and polymer concentration in the reactor, the optimization handles these very well with only very small fluctuations.

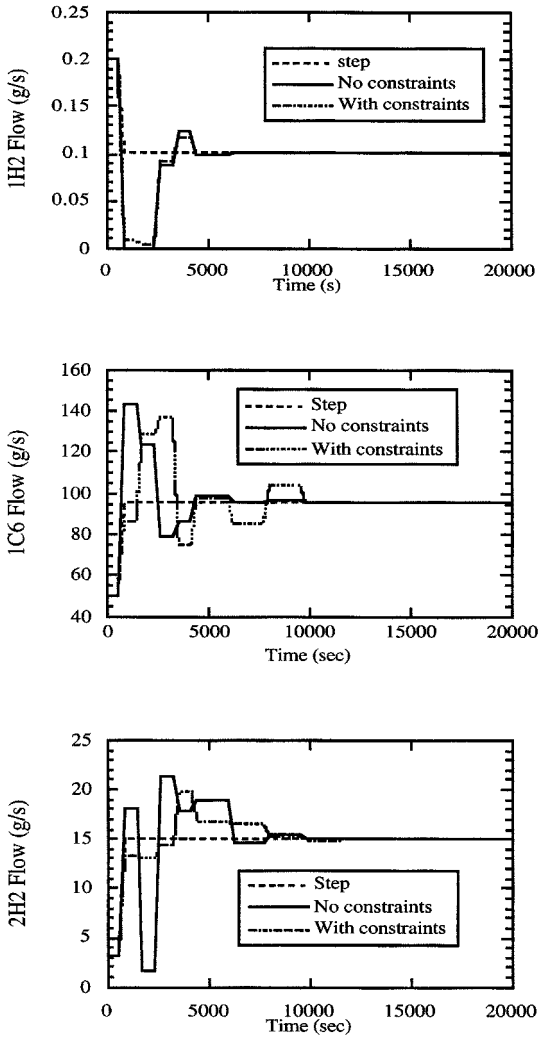

Figure 12. Results of difficult grade transition—(4).

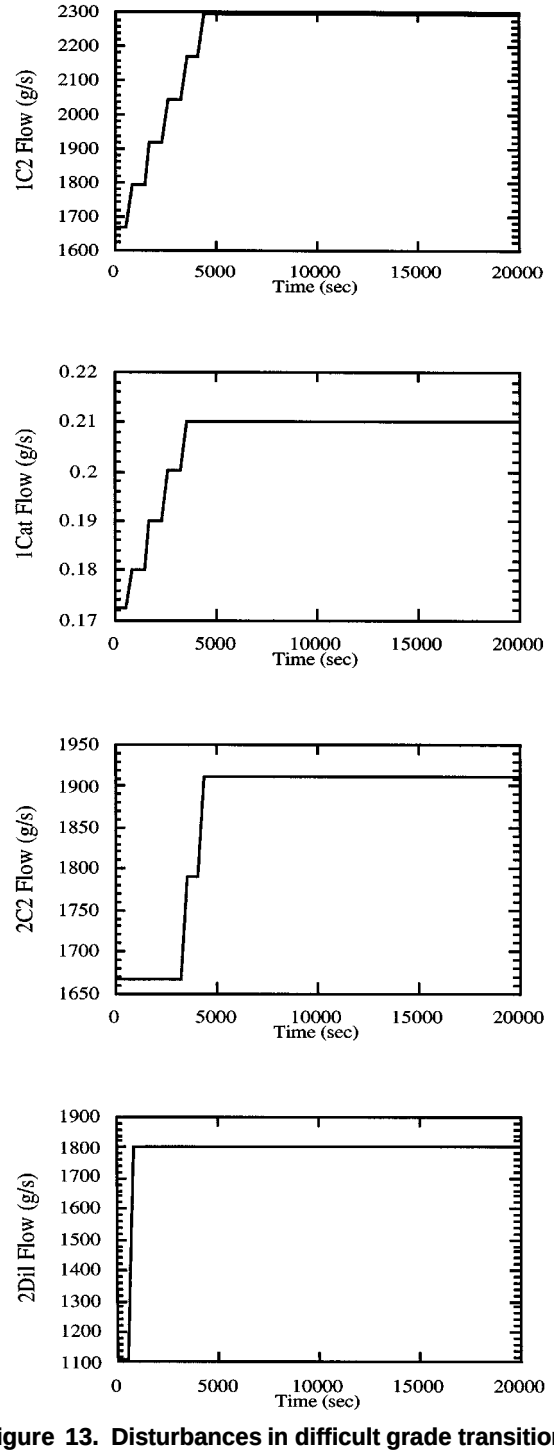

Figure 13. Disturbances in difficult grade transition.

As described before, some constraints are imposed during grade transition because of plant safety and/or property protection. In this simulation an upper constraint for the increasing rate of the production rate in the first reactor is imposed for the following reasons: (1) because the volume of the first reactor is much smaller than the second one (volume ratio is one to three), the temperature control for the first reactor is very sensitive; hence it is very important to have a slow increase in the production rate in order to avoid reactor runaway; (2) in the first reactor, the hydrogen flow is decreased in order for the number-average molecular weight to be increased, and the hexene flow is increased in order for polymer density to be decreased. This results in an increase in catalyst productivity, because catalyst inhibition by hydrogen is decreased and the catalyst activation reaction by hexene is increased. (3) The ethylene flow is greatly increased in the first reactor so that the polymerization reaction rate is greatly increased. The upper constraint of the increasing rate of the production rate in the first reactor is set to 130 g/s for 5 min.

There are some significantly different results from the case of unconstrained optimization. The rate of the production in the first reactor increases more slowly than the unconstrained case because of the constraint. In order to satisfy the constraint, the hydrogen flow and hexene flow to the first reactor are different from the unconstrained case. The hydrogen flow to the first reactor is not set to zero, and the hexene flow is not set to the upper-bound value after starting the grade transition. Therefore, the dynamics of the number-average molecular weight and polymer density in the first reactor are slower than those of the unconstrained case.

The hydrogen flow to the second reactor is synchronized with the changes in the first reactor's product. The hydrogen flow is not increased to the upper bound at the beginning of grade transition, but after stabilizing the first reactor's production rate, it goes to the upper bound.

As was the case for the difficult grade transition, it is more beneficial to conduct grade-transition optimization for constrained grade transitions because less obvious, yet effective strategies are obtained.

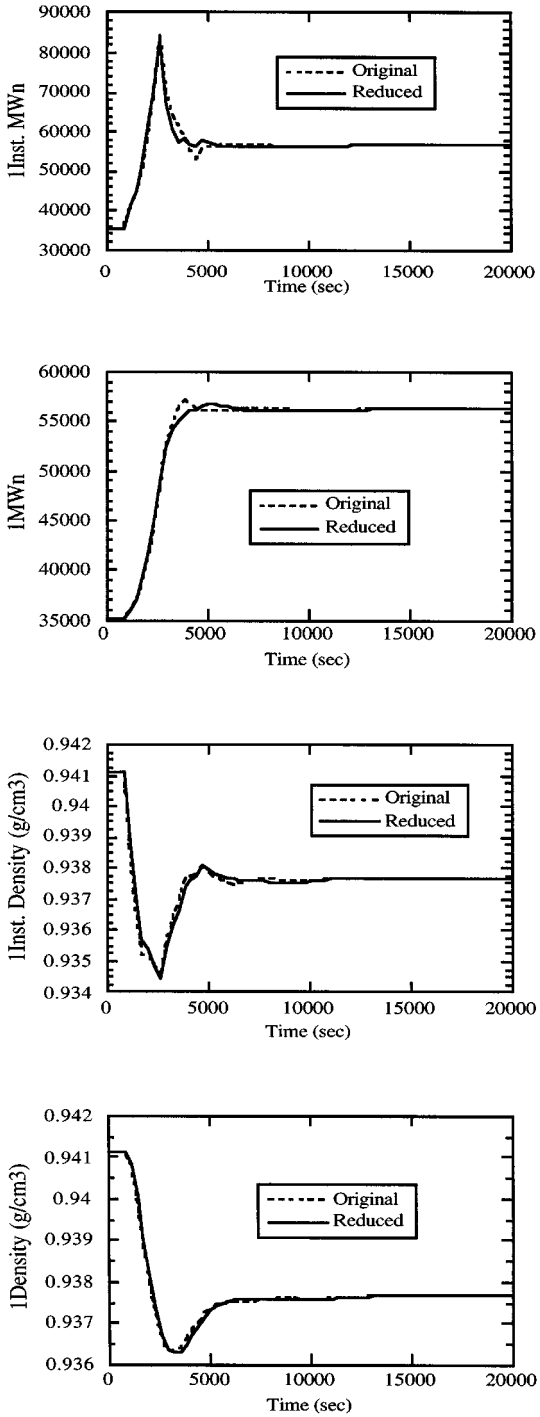

Figure 14. Results of reduced inputs—(1).

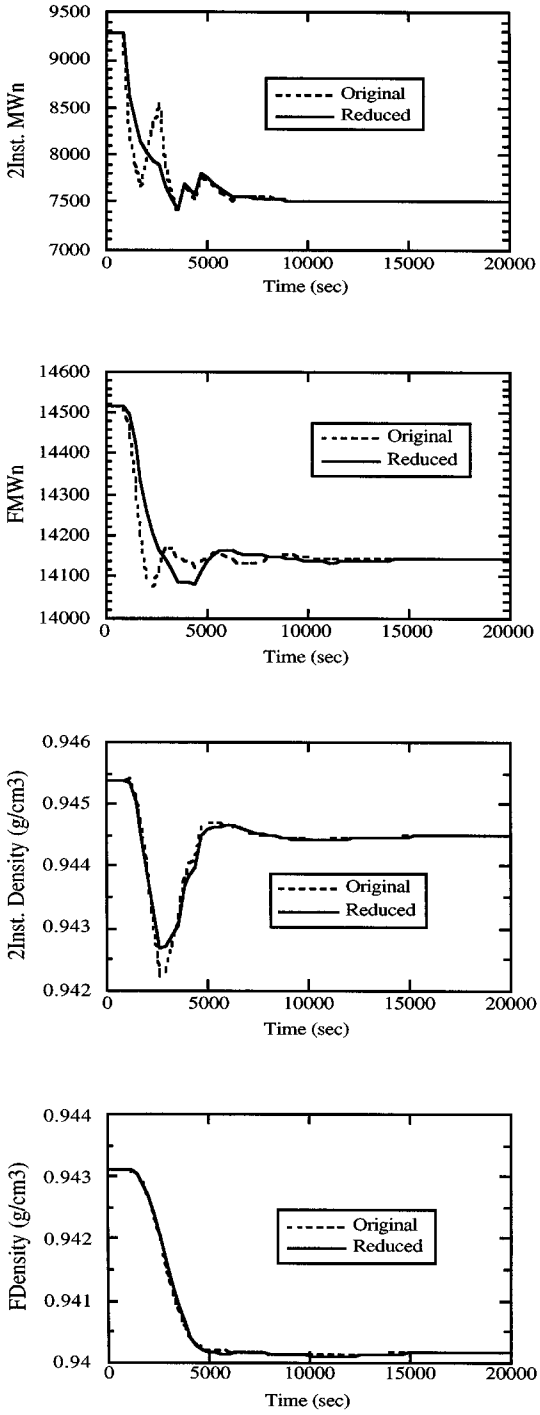

Figure 15. Results of reduced inputs—(2).

Reducing decision variables

When optimal grade-transition strategies are installed in an actual plant, it is better to have a simple strategy. Therefore, in this section simulation by using a simple input parameterization that is defined by dashed lines in Figure 4 is performed for grade transition 2 with no constraints. The initial values for the input parameters u_{ij} is decided by the original results of the unconstrained optimization performed. In this simulation, the number of the input parameters (input

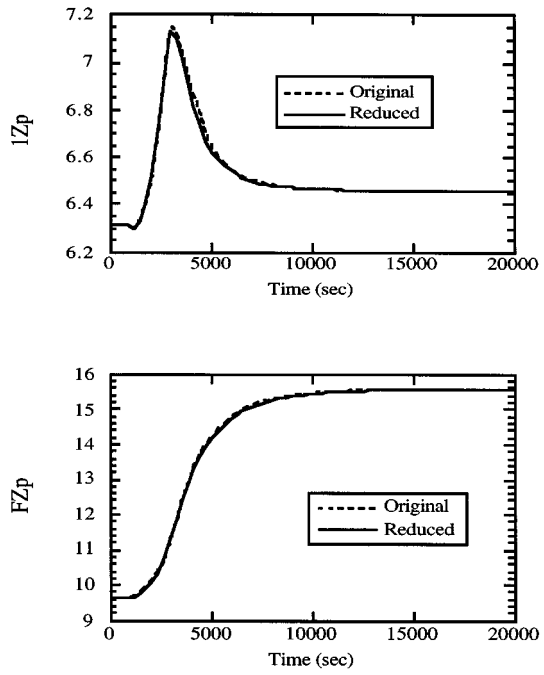

Figure 16. Results of reduced inputs—(3).

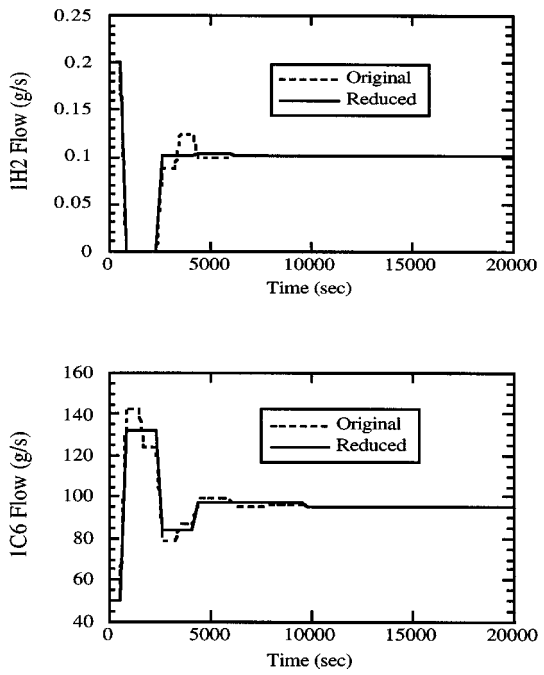

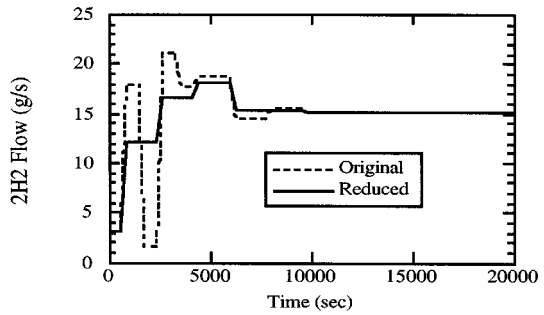

Figure 17. Results of reduced inputs—(4).

time intervals) is reduced from 20 to 10. The results are shown by the solid lines in Figures 14–17. In order to easily compare the results, the original optimization results are shown by dashed lines in the same figures.

Although very similar results to those of original optimization are obtained in these simulations, the dynamics of the number-average molecular weight of the final product is slower than the original simulation. At the beginning of the grade transition, the hydrogen flow is overshot and undershot, but the average value of the first two inputs of the original optimized values of the hydrogen flow is set in this simulation. This leads to the different dynamics of the number-average molecular weight of the final product. Clearly, if additional intervals were allowed for this hydrogen flow, almost identical results would be obtained in a reduced parameter optimization as for the original. Because the other product dynamics are the same as the original one, this method is very useful for installing in actual plants.

Optimization considering a product band

In all previous simulations the objective function, Eq. 4 was used, but in this case the objective function, Eq. 5, which considers a product band, is used. The optimization is conducted for grade transition 1 without constraints. The results are shown in Figures 18–21. In these figures, the optimization results where the previous objective function, Eq. 4, is used are also included in order to compare the results easily. The values of the product band for the number-average molecular weight are $\pm 10\%$ of the target values and ± 0.0005 for polymer density.

Some interesting results are obtained; for example, the number-average molecular weight in the first reactor stops decreasing as soon as it goes into the product band. This is because the hydrogen in the second reactor must be discharged in order to increase the molecular weight and it is not easy to do this as explained before; hence, the first reactor hydrogen flow stops increasing in order for the hydrogen concentration in the second reactor to quickly decrease. In addition, polymer density stops decreasing as soon as it enters the product band. The more feed of hexene to the reactor in order to decrease polymer density makes the number-average molecular weight decrease. This is the reverse of the desired dynamics. Because the dynamics of increasing the instantaneous number-average molecular weight is very slow, the density dynamics helps this to increase more rapidly. Accordingly, the results of the number-average molecular weight in the final product by using this objective function is better than the previous one, although the difference is very small. In this simulation, the volume of the second reactor is three times as large as that of the first reactor, and the hydrogen flow to the first reactor is much less than that of the second reactor. Therefore, improvement using the new objective function is not so significant, but if the hydrogen flow to the first reactor was not so small, a greater improvement would be obtained by using this objective function.

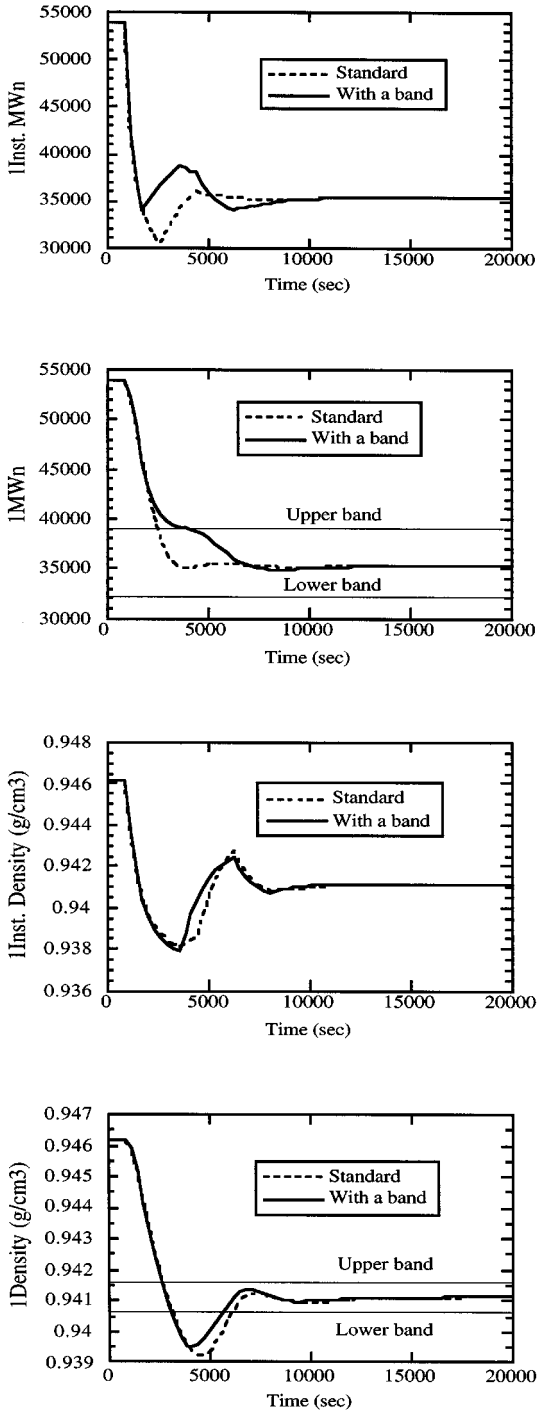

Figure 18. Results of optimization considering a product band—(1).

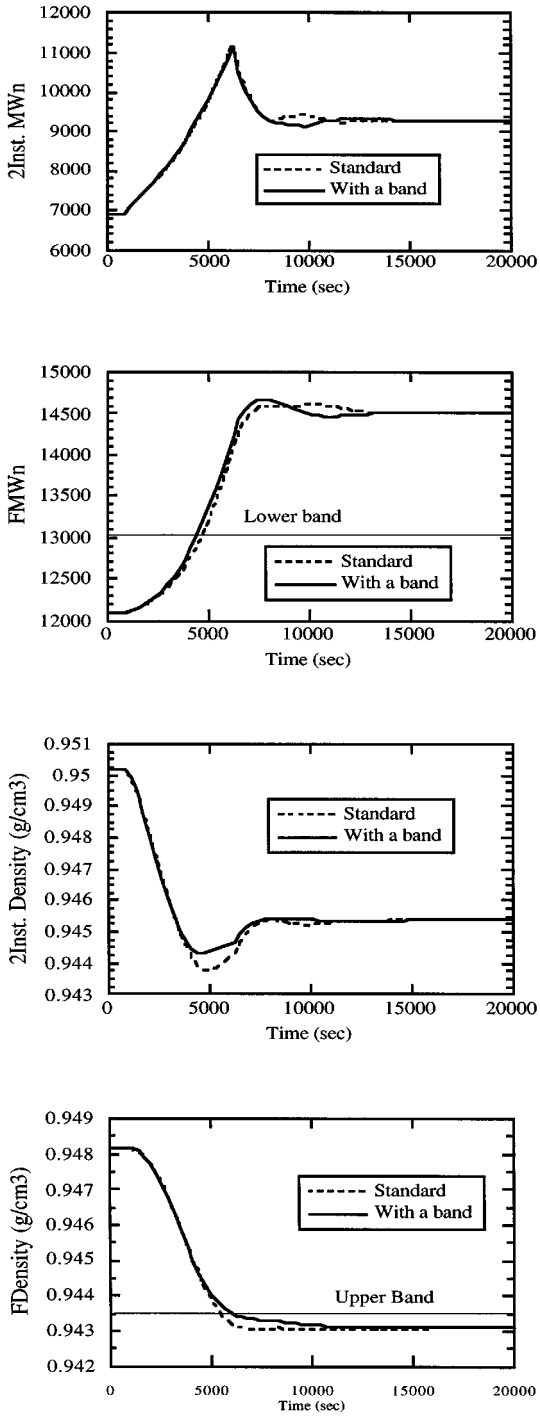

Figure 19. Results of optimization considering a product band—(2).

Conclusions

In this article the optimization of grade transitions in multistage loop reactors with bimodal products was simulated by using the control-vector parameterization method. This was performed by connecting the polymerization-process simulator, POLYRED, with a sequential quadratic programming in MATLAB. The two main grade-transition examples, an easy case (all other inputs except the hexene and hydrogen flow to the first reactor and the hydrogen to the second reactor, were constant) and a difficult case (every input was changed during grade transition), were simulated with no constraints and with constraints on the states. They were also compared with simple step-change operations.

First of all, results show the validity of the control-vector parameterization method to olefin polymerization multistage reactors. By using SQP as the NLP solver, constraints of states

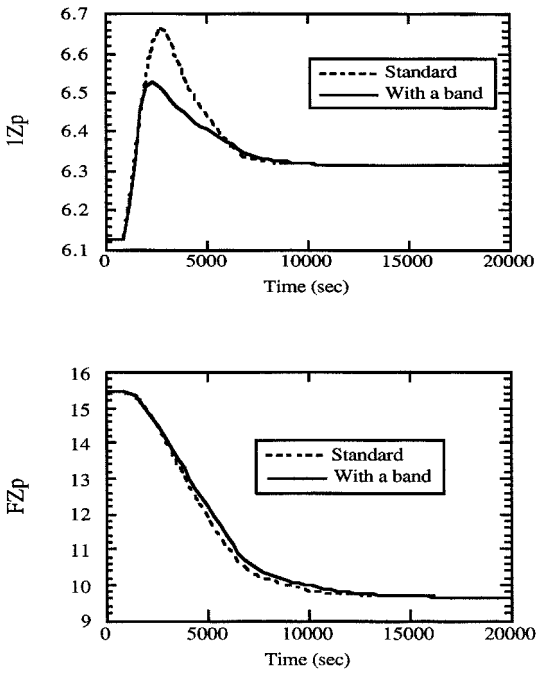

Figure 20. Results of optimization considering a product band—(3).

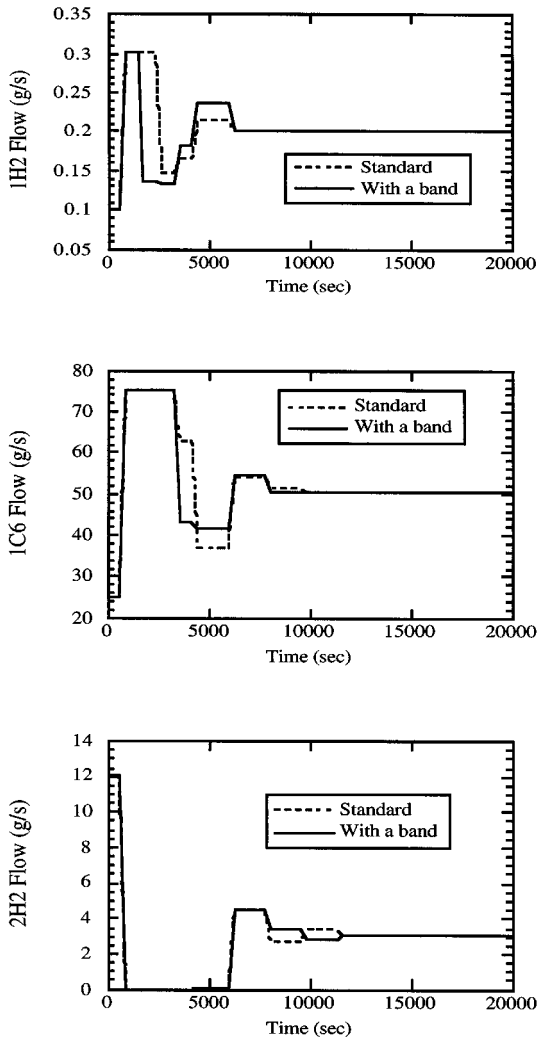

Figure 21. Results of optimization considering a product band—(4).

can be easily installed and stable solutions were obtained. One advantage of the method in this article is that any constraint can be easily installed in the optimization. Another advantage is that this method can be easily applied to other reactors by changing the model in the process simulator.

Several optimized grade-transition operations were compared. Clearly, the optimized results were much better than the step-change operations in every case. If each result is compared with the step-change operation, the easy grade-transition case with no constraint obtained the best improvement with regard to grade-transition time. However, the solutions of each controlled variable were simple overshoot and/or undershoot strategies that can be prediced without using optimization. Actually, in most industrial plants, these types of overshoot and/or undershoot operations are normally performed by analyzing the actual grade-transition data obtained by plant operators. On the other hand, the unconstrained and constrained cases of difficult grade transition are not easy to predict without using optimization algorithms. Therefore, the value of performing grade-transition optimization for these types of grade transition is much greater than the unconstrained easy grade-transition case. Let us illustrate the economic benefits assuming product bands of $\pm 10\%$ in MW_n and ± 0.0005 in density. For the case of the easy grade transition with constraints, there was a 30% reduction in transition time and the amount of off-spec product compared with the simple step-change operation. For the difficult grade-transition case with constraints, there was a 40% improvement in transition time and amount of off-spec product.

An attempt to reduce the number of time intervals in the decision variables was made. Practically, reducing the decision variables makes it easier to install an actual control strategy in a plant. It was shown that reducing decision variables is possible by rearranging the input parameterization after obtaining more complex optimal solutions.

Finally, objective functions were used that also considered property bands during grade transitions. Although this new objective function is not useful for every case, better results than by using the standard objective function can be obtained for some types of grade transitions.

In practice, in order to greatly improve grade transition, the optimization should be performed on-line. Even if the optimal solution is obtained by off-line methods, the actual response of the plant may be different from the model because of disturbances; hence, plant dynamics may deviate from the calculated optimal outputs. One solution for this is that the model should be adaptively updated regularly (for example, using state corrections at intervals based on plant measurements) and then used to recalculate the optimization at several points during the grade transition. However, the optimization calculations can take some time. Therefore, the optimization problem should be made as simple as possible in order to reduce the calculation time. Reducing the number of decision variables as in this article may be one solution

for this. Another solution might be streamlining the model and model updating calculations as much as possible while maintaining model fidelity. It is clear that the implementation of on-line optimization of grade transition strategies remains a very challenging area.

Acknowledgments

The authors are indebted to the U.S. Dept. of Energy, to Showa Denks, K. K., and to the sponsors of the University of Wisconsin Polymerization Research Engineering Laboratory for support of this research.

Literature Cited

Debling, J. A., G. Han, F. Kuijpers, J. Verbury, J. Zacca, and W. H. Ray, "Dynamic Modeling of Product Grade Transitions for Olefin Polymerization Processes," *AIChE J.*, **40**, 506 (1994).

Grace, A., "Optimization Toolbox for Use with MATLAB, MATLAB User's Guide (November 1992)," The MATH WORKS, Natick, MA (1992).

Karol, F. J., S.-C. Kao, and K. J. Cann, "Comonomer Effects with High-Activity Titanium and Vanadium Catalysts," *J. Poly. Sci.: Part A: Poly. Chem.*, **31**, 2541 (1993).

McAuley, K. B., and J. F. MacGregor, "Optimal Grade Transitions in a Gas Phase Polyethylene Reactor," *AIChE J.*, **38**, 1564 (1992).

Ogunnaike, B. A., and W. H. Ray, *Process Dynamics, Modeling and Control*, Oxford Univ. Press, New York (1994).

Ohshima, M., et al., "Grade Transition Control for an Impact Copolymerization Reactor," IFAC Symp. ADCEM '94, Kyoto, Japan, p. 507 (1994).

Ramanathan, S., and W. H. Ray, "The Dynamic Behavior of Polymerization Process Flowsheets," Eng. Foundation Conf. on Polymer Reaction Engineering, Santa Barbara, CA (1991).

Ray, W. H., "On the Mathematical Modeling of Polymerization Reactors," *J. Macromol. Sci.-Rev. Macromol. Chem. Phys.*, **C8**, 1 (1972).

Ray, W. H., and J. Szekely, *Process Optimization*, Wiley, New York (1973).

Shaffer, W. K. A., and W. H. Ray, "Polymerization of Olefins Through Heterogeneous Catalyst: XVIII. A Kinetic Explanation for Unusual Effects," *J. Appl. Poly. Sci.*, **65**, 1053 (1997).

UWPREL, "POLYRED: Computer-Aided POLYmerization REactor Design, User's Manual Version 4.1," University of Wisconsin-Madison, Madison (1997).

Zacca, J. J., and W. H. Ray, "Modelling of the Liquid Phase Polymerization of Olefins in Loop Reactors," *Chem. Eng. Sci.*, **48**, 3743 (1993).

Appendix: Summary of Mathematical Model

In this Appendix the kinetic model for Ziegler-Natta catalyst polymerization reactions with two sites is explained. In the following the superscript k shows the catalyst site ($k = 1$ or 2).

The catalyst sites consist of potential sites (C_{pot}), activated sites, and dead sites (C_d). There are two different activated sites: one is a growing site ($P^k_{n,j}$) and another is a vacant site (P_0). The term $P^k_{n,j}$ denotes a live (growing) polymer chain at a catalyst site of type k with an activated end-group j. The term D^k_n refers to dead polymer produced at site k by deactivation or chain transfer. The chain length of a copolymer molecule is denoted by vector $n = [n_1, n_2]^T$, where n_1 is the chain length of monomer (ethylene) and n_2 is the chain length of comonomer (hexene). The terms C_H, C_{M_1}, C_{M_2}, C_A denote the concentrations of hydrogen, ethylene, hexene, cocatalyst, respectively. The following are the detailed kinetics that are considered in the dynamic-process simulator.

1. Site activation reactions
   By cocatalyst (A)

$$C_{\text{pot}} + A \xrightarrow{k^k_{aA}} P^k_0 + B \qquad R^k_{aA} = k^k_{aA} C_{\text{pot}} C_A$$

   By comonomer (M_2)

$$C_{\text{pot}} + M_2 \xrightarrow{k^k_{aM_2}} P^k_0 + M_2 \qquad R^k_{aM_2} = k^k_{aM_2} C_{\text{pot}} C_{M_2}.$$

2. Chain initiation reactions
   By monomer and comonomer (M_i)

$$P^k_0 + M_i \xrightarrow{k^k_{pi}} P^k_{\boldsymbol{\delta}_i, i} \qquad R^k_{pi} = k^i_{pi} P^k_0 C_{Mi}.$$

3. Chain propagation reactions
   By monomer and comonomer (M_i)

$$P^k_{n,j} + M_i \xrightarrow{k^k_{pij}} P^k_{n+\boldsymbol{\delta}_i, i} \qquad R^k_{pij} = k^k_{pij} \mu^k_{0,j} C_{Mi}$$

where

$$\mu^k_{0,j} = \sum_{n=0}^{\infty} P^k_{n,j}.$$

4. Chain transfer reactions
   By hydrogen (H_2)

$$P^k_{n,j} + H_2 \xrightarrow{k^k_{cHj}} D^k_n + P^k_0 \qquad R^k_{cHj} = k^k_{cHj} \mu^k_{0,j} (C_H)^{0.5}$$

   By cocatalyst (A)

$$P^k_{n,j} + A \xrightarrow{k^k_{cAj}} D^k_n + P^k_0 \qquad R^k_{cAj} = k^k_{cAj} \mu^k_{0,j} (C_A).$$

   By monomer and comonomer (M_i)

$$P^k_{n,j} + M_i \xrightarrow{k^k_{cMij}} D^k_n + P^k_{\boldsymbol{\delta}_i, i} \qquad R^k_{cMij} = k^k_{cMij} \mu^k_{0,j} C_{Mi}$$

   Spontaneous

$$P^k_{n,j} \xrightarrow{k^k_{cSpj}} D^k_n + P^k_0 \qquad R^k_{cSpj} = k^k_{cSpj} \mu^k_{0,j}.$$

5. Site deactivation reactions
   Spontaneous

$$P^k_o \xrightarrow{k^k_{dSp}} C_d \qquad R^k_{dSp} = k^k_{dSp} \sum_j{}' \mu^k_{0,j}$$

$$P^k_{n,j} \xrightarrow{k^k_{dSp}} C_d + D^k_n.$$

By using population balances for the polymer species and mass balances for the nonpolymer species over the kinetics described earlier, a nonstationary model for the dynamic rate of change of the polymer properties, which are controlled during grade transitions, can be calculated. This model is called the population balance model, and the detailed deriva-

tion of this model is given in Ray (1972). As described before, the main controlled properties during grade transition are the number-average molecular weight, polydispersity, and polymer density. The cumulative values of these properties in the reactor are calculated, as are the instantaneous values.

The population balances yield the rates of change of the concentrations of all the polymers that have different chain lengths. By using the following moments, these rates of change are transformed to a set of equations including the kinetic rates of change of the polymer moments. In the population-balance model the following polymer moments are defined and the basic polymer properties can be calculated by using these polymer moments.

First, the live polymer fth moments at site type k are defined as

$$\mu^k_{f,j} = \sum_{n=\mathbf{0}}^{\infty} n^f P^k_{n,j} \qquad \text{with end-group } j$$

$$\mu^k_f = \sum_{j=1}^{2} \mu^k_{f,j} \qquad \text{summed over end-group type}$$

$$\mu_f = \sum_{k=1}^{2} \mu^k_f \qquad \text{summed over site and end-group type.}$$

Second, the bulk, which is live and dead, polymer fth moments at site type k are

$$\lambda^k_f = \sum_{n=\mathbf{0}}^{\infty} n^f \left(\sum_{j=1}^{2} P^k_{n,j} + D^k_n \right).$$

Here, f is a vector whose elements corresponds to the monomeric group. Because two monomers are considered in this sample process, the vector f has two elements. For the first moment with respect to monomeric group 1 (in this research, ethylene), f is defined as [1 0]. Similarly for the first moment with respect to monomeric group 2 (hexene), f is [0, 1].

By using the kinetics and these polymer live and bulk moments, several important factors and cumulative and instantaneous properties of polymers can be calculated as follows:

1. Production rate

At site type k

$$\text{Product}^k = \sum_{i=1}^{2} \sum_{j=1}^{2} R^k_{pij}$$

Overall

$$\text{Product} = \sum_{k=1}^{2} \sum_{i=1}^{2} \sum_{j=1}^{2} R^k_{pij}$$

Ratio at site type k

$$\text{ProRatio}^k = \frac{\text{Product}^k}{\text{Product}}.$$

2. Copolymer composition (mole fraction) at site type k

Live polymer

$$LFp^k_i = \frac{\mu^k_{\boldsymbol{\delta}_i}}{\sum_{i=1}^{2} \mu^k_{\boldsymbol{\delta}_i}}$$

Bulk polymer

$$Fp^k_i = \frac{\lambda^k_{\boldsymbol{\delta}_i}}{\sum_{i=1}^{2} \lambda^k_{\boldsymbol{\delta}_i}}.$$

3. Weight fraction of bulk polymer that is produced at site type k

$$Wp^k = \frac{\sum_{i=1}^{2} Mw(i) \lambda^k_{\boldsymbol{\delta}_i}}{\sum_{k=1}^{2} \sum_{i=1}^{2} Mw(i) \lambda^k_{\boldsymbol{\delta}_i}}$$

where $Mw(i)$ is a molecular weight of monomer i.

4. Number-average molecular weight at site type k

Live polymer at site type k

$$LMWn^k = \frac{\sum_{i=1}^{2} Mw(i) \mu^k_{\boldsymbol{\delta}_i}}{\mu^k_{\mathbf{0}}}$$

Bulk polymer at site type k

$$MWn^k = \frac{\sum_{i=1}^{2} Mw(i) \lambda^k_{\boldsymbol{\delta}_i}}{\lambda^k_{\mathbf{0}}}.$$

5. Overall number average molecular weight

Instantaneous

$$IMWn = \frac{1}{\sum_{k=1}^{2} \frac{\text{ProRatio}^k}{LMWn^k}}$$

Cumulative

$$MWn = \frac{1}{\sum_{k=1}^{2} \frac{Wp^k}{MWn^k}}.$$

6. Polydispersity

$$Zp = \frac{\lambda_2 \lambda_0}{(\lambda_1)^2}$$

7. Polymer density at site type k

Live polymer at site type k

$$L\rho^k = a_1 + a_2\left(LFp_2^k\right) + a_3\left(LFp_2^k\right)^2 + a_4\left(LFp_2^k\right)^3$$

Bulk polymer at site type k

$$\rho^k = a_1 + a_2\left(Fp_2^k\right) + a_3\left(Fp_2^k\right)^2 + a_4\left(Fp_2^k\right)^3$$

where $a_1 \sim a_4$ are constants.

8. Overall polymer density

Instantaneous

$$I\rho = \sum_{k=1}^{2} \mathrm{ProRatio}^k L\rho^k$$

Cumulative

$$\rho = \sum_{k=1}^{2} Wp^k \rho^k.$$

In applying the bimodal reactors, these polymer properties can be calculated independently for both reactors. For example, the number-average molecular weight has the following four different items.

1. Instantaneous number-average molecular weight in the first reactor
2. Cumulative number-average molecular weight in the first reactor
3. Instantaneous number-average molecular weight in the second reactor
4. Cumulative number-average molecular weight in the second reactor.

Since the product in the second reactor can be regarded as the final product of the bimodal reactors, cumulative values in the second reactor will be referred to as final product values.

The main polymer properties that should be considered during grade transitions can be obtained in the aforementioned calculations. Since moment equations are the nonstationary model for the dynamic rates of change of polymer properties, the model of the main polymer properties obtained here can show the dynamics during grade transitions.

Manuscript received Oct. 6, 1998, and revision received May 26, 1999.